

# Molecular Dynamics Simulations of Microscopic Structural Transition and Macroscopic Mechanical Properties of Magnetic Gels

Xuefeng Wei,<sup>†,‡</sup> Gaspard Junot,<sup>¶</sup> Ramin Golestanian,<sup>§,||</sup> Xin Zhou,<sup>‡,†</sup> Yanting  
Wang,<sup>⊥,†,‡</sup> Pietro Tierno,<sup>¶,#,@</sup> and Fanlong Meng<sup>\*,⊥,†,‡</sup>

<sup>†</sup>*Wenzhou Institute, University of Chinese Academy of Sciences, Wenzhou, Zhejiang  
325000, China*

<sup>‡</sup>*School of Physical Sciences, University of Chinese Academy of Sciences, 19A Yuquan  
Road, Beijing 100049, China*

<sup>¶</sup>*Departament de Física de la Matèria Condensada, Universitat de Barcelona, 08028  
Barcelona, Spain*

<sup>§</sup>*Max Planck Institute for Dynamics and Self-Organization (MPIDS), D-37077 Göttingen,  
Germany*

<sup>||</sup>*Rudolf Peierls Centre for Theoretical Physics, University of Oxford, Oxford OX1 3PU,  
United Kingdom*

<sup>⊥</sup>*CAS Key Laboratory of Theoretical Physics, Institute of Theoretical Physics, Chinese  
Academy of Sciences, Beijing 100190, China*

<sup>#</sup>*Universitat de Barcelona Institute of Complex Systems, 08028 Barcelona, Spain*

<sup>@</sup>*Institut de Nanociència i Nanotecnologia, Universitat de Barcelona, 08028 Barcelona,  
Spain*

E-mail: fanlong.meng@itp.ac.cn

## Abstract

Magnetic gels with embedded micro/nano-sized magnetic particles in crosslinked polymer networks can be actuated by external magnetic fields, with changes in their internal microscopic structures and macroscopic mechanical properties. We investigate the responses of such magnetic gels to an external magnetic field, by means of coarse-grained molecular dynamics simulations. We find that the dynamics of magnetic particles are determined by the interplay of between magnetic dipole-dipole interactions, polymer elasticity and thermal fluctuations. The corresponding microscopic structures formed by the magnetic particles such as elongated chains can be controlled by the external magnetic field. Furthermore, the magnetic gels can exhibit reinforced macroscopic mechanical properties, where the elastic modulus increases algebraically with the magnetic moments of the particles in the form of  $\propto (m - m_c)^2$  when magnetic chains are formed. This simulation work can not only serve as a tool for studying the microscopic and the macroscopic responses of the magnetic gels, but also facilitate future fabrications and practical controls of magnetic composites with desired physical properties.

## Introduction

Magnetic gels, with micro/nano-sized magnetic particles embedded in crosslinked polymeric gels, belong to the class of smart magnetic materials, whose physical properties can be controlled by external magnetic fields.<sup>1-3</sup> By tuning such fields, e.g., the direction, the strength or the frequency, one can change the materials with different mechanical responses, such as material stiffness<sup>4-7</sup> and deformations.<sup>8-10</sup> Based on such field-controlling features, magnetic gels have been fabricated in laboratories and used as magnetic robots,<sup>11-13</sup> sensors,<sup>14-16</sup> actuators,<sup>17,18</sup> etc., and also for bio-medical applications<sup>19-21</sup> such as drug delivery/release due to the bio-friendly characteristics of magnetic fields.

Under an applied magnetic field, the materials can respond in different ways depending

on how the magnetic particles are embedded in the polymer matrix. For magnetic particles able to move freely in the polymer gel, they can form microscopic chains when the magnetic dipole-dipole interactions between particles dominate the thermal fluctuation as in ordinary solutions,<sup>22,23</sup> where the polymer gel serves mainly as a viscoelastic medium without much changes in its mechanical properties. For superparamagnetic particles fixed in the polymer network,<sup>24</sup> the particles can still move but now they induce microscopic distortions in the polymer network, and they can even form magnetic chains if the magnetic dipole-dipole interactions are strong enough. In the latter case, the responses of the embedded particles to the external magnetic field with simultaneous deformations of the polymer network underpins the physical mechanism for controlling the mechanical properties of the magnetic gels.

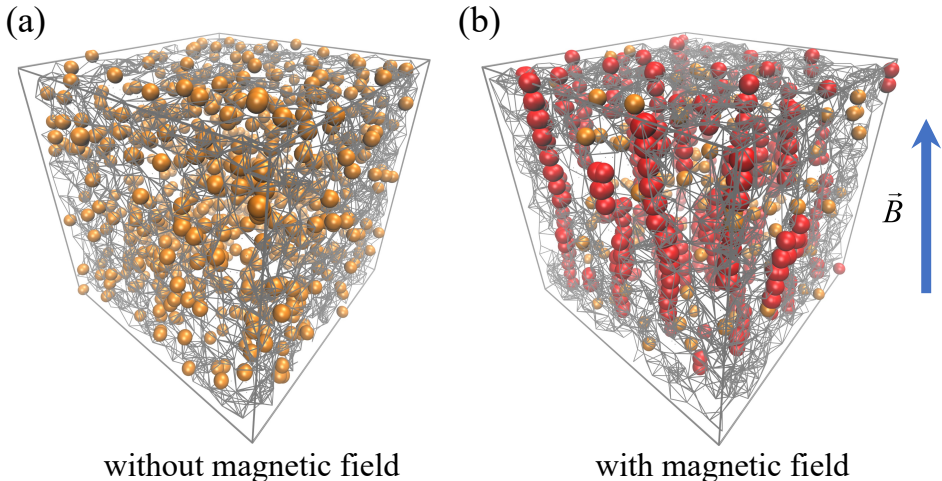


Figure 1: Magnetic gels with (a) uniformly distributed magnetic particles without the magnetic field and (b) magnetic chains under an external magnetic field. Spheres denote the magnetic particles and grey lines denote partial connections in the polymer network.

The connection between the microscopic motion of the magnetic particles and the macroscopic responses of the material, is the key for understanding how external magnetic fields can be utilised to control the material properties. Experimental methods such as small-angle X-ray scattering (SAXS),<sup>25</sup> small angle neutron scattering (SANS),<sup>26</sup> electron magnetic resonance (EMR),<sup>27</sup> etc., are utilised for detecting the internal structure of the magnetic gels with macroscopic mechanical properties which are measurable by tensile testing,<sup>28,29</sup> dynamic

mechanical analysis,<sup>30,31</sup> etc. Theoretical attempts include analytical modelling such as the lattice models<sup>32,33</sup> and continuum models,<sup>24,34,35</sup> and numerical methods such as finite element calculations,<sup>36</sup> Monte Carlo simulations<sup>37,38</sup> and molecular dynamics simulations.<sup>39–41</sup> In this work, we use coarse-grained molecular dynamics simulations to investigate the microscopic motion and structures of the magnetic particles, together with the macroscopic mechanical properties especially about the anisotropic elasticity of the materials.

## Simulation methodology

*Polymer network.* We follow Ref.42 to construct the 3D packing-derived (PD) polymer network. We first randomly place  $N = W^3$  radially bidisperse spheres with harmonic repulsive interactions within a cubic unit cell of side length  $W$  ( $W = 20$  is taken in later discussions), where half of the spheres are assigned with radius  $r = r_0$  and the other half with  $r = \nu r_0$  ( $\nu = 1.4$  is chosen to avoid long-range crystal order<sup>42–44</sup>). By continuously increasing the radius  $r_0$  from  $r_0 = 0$ , the spheres will reach a jammed state at  $r_0^J$ . Then, from this disordered packing state, we generate a contact network by connecting the centers of the overlapping spheres (excluding rattlers) with springs at their rest lengths and angles. For sufficiently large systems, this procedure generates contact networks with the connectivity  $z = 2d$ , where  $d$  is the system dimensionality. After generating the underlying network structure, we remove randomly chosen bonds and any consequent dangling ends repeatedly until the network reaches the desired average connectivity  $z$ . The bonds connecting neighbouring nodes are modelled as Hookean springs and the bending effects is considered by introducing the bending energy. The stretching and the bending energy of the network can be written as:

$$U_{\text{stretching}}(r) = \frac{\mu}{2} \sum_{i,j} \frac{(r_{ij} - r_{ij,0})^2}{r_{ij,0}}, \quad (1)$$

$$U_{\text{bending}}(r) = \frac{\kappa}{2} \sum_{ijk} \frac{(\theta_{ijk} - \theta_{ijk,0})^2}{l_{ijk,0}}, \quad (2)$$

respectively, where  $\mu$  and  $\kappa$  denote the Hookean constant and the bending rigidity, respectively,  $r_{ij,0}$  and  $r_{ij}$  denote the length of spring ( $ij$ ) connecting the  $i$ th and the  $j$ th node before and after stretching, respectively,  $\theta_{ijk,0}$  and  $\theta_{ijk}$  denote the angles between the spring ( $ij$ ) and ( $jk$ ) before and after bending, respectively, and  $l_{ijk,0} = (r_{ij,0} + r_{jk,0})/2$  denotes the average length of the two connecting springs.

*WCA potential.* We choose polymer nodes randomly with the number density  $n_0$  to be replaced with magnetic particles, i.e., the magnetic particles are uniformly distributed in the prepared state. The diameters of the magnetic particles are set as  $\sigma_m = 1.0\sigma$  and other non-magnetic nodes are set as  $\sigma_n = 0.2\sigma$ . In our simulations, the truncated Weeks-Chandler-Andersen (WCA) potential<sup>45</sup> is used to simulate the non-bonded and non-magnetic interactions between particles, as:

$$U(r) = \begin{cases} 4\epsilon \left[ \left(\frac{\sigma_{ij}}{r}\right)^{12} - \left(\frac{\sigma_{ij}}{r}\right)^6 \right] + C & \text{if } r \geq r_{\text{cutoff}}, \\ 0 & \text{if } r < r_{\text{cutoff}}, \end{cases}$$

where  $r_{\text{cutoff}} = 2^{1/6}\sigma_{ij}$  is the cutoff distance for given pairs,  $\sigma_{ij} = (\sigma_i + \sigma_j)/2$  is the average diameter of particle  $i$  and  $j$ , and  $C$  is a constant ensuring the continuity of the potential energy at the cutoff distance. In this work we take  $\epsilon$  and  $\sigma$  as the unit energy and length, respectively.

*Magnetic dipole-dipole interactions.* The superparamagnetic particles can be magnetized under an external magnetic field  $\mathbf{B}_{\text{ext}}$ , and they acquire magnetic moments  $\mathbf{m} = \chi v_p \mathbf{B}_{\text{ext}}/\mu_0$  pointing along the direction of the magnetic field, where  $\chi$  is the magnetic susceptibility,  $v_p$  is the particle volume and  $\mu_0$  is vacuum permeability. These magnetic particles possess moments aligned along the field direction, and the interactions between the magnetic particles are:

$$U_{\text{dd}}(\mathbf{r}_{ij}) = \frac{\mu_0}{4\pi} \left[ \frac{1}{r_{ij}^3} (\mathbf{m}_i \cdot \mathbf{m}_j) - \frac{3}{r_{ij}^5} (\mathbf{m}_i \cdot \mathbf{r}_{ij})(\mathbf{m}_j \cdot \mathbf{r}_{ij}) \right]. \quad (3)$$

The magnetic dipole-dipole interactions between magnetic particles can be either attractive or repulsive, depending on their relative locations with respect to the separation  $\mathbf{r}_{ij}$ .

*Molecular dynamics simulations.* We perform the molecular dynamics simulations on a coarse-grained level based on the above model setup, using LAMMPS software.<sup>46</sup> The simulations are done in the canonical  $NVT$  ensemble using a Langevin thermostat.<sup>47,48</sup> The equation of motion for each particle is:

$$m\ddot{\mathbf{r}} = -\gamma\dot{\mathbf{r}} + \mathbf{F} + \boldsymbol{\xi}, \quad (4)$$

where  $m$  denotes the mass of the particle,  $\gamma$  denotes the friction constant,  $\mathbf{F}$  denotes the forces exerted by other particles and the polymer network, and  $\boldsymbol{\xi}$  denotes the thermal noise due to the random collisions with implicit solvent molecules, which obeys fluctuation-dissipation theorem. Periodic boundary conditions are adopted in the simulations and the detailed simulation procedure including simulation parameters can be found in the supplement.<sup>49</sup>

## Results and discussions

### Internal microscopic structures

The elastic properties, e.g., the shear modulus and the bulk modulus, of the magnetic gels before applying any external magnetic field can be controlled by changing the connectivity in the polymer networks, as shown in Fig. 2(a). By increasing the connectivity of the polymer network, both the shear and the bulk modulus will increase, in an approximate form of  $\propto (z - z_c)^3$  with  $z_c \simeq 3.2$  as the critical connectivity for the polymer network to exhibit finite elasticity.<sup>42,50</sup>

As shown in Fig. 2(b), the magnetic particles can form chain-like structures by increasing the strength of the magnetic field (magnetic moments of superparamagnetic particles), when the magnetic dipole-dipole interactions between the magnetic particles dominate the

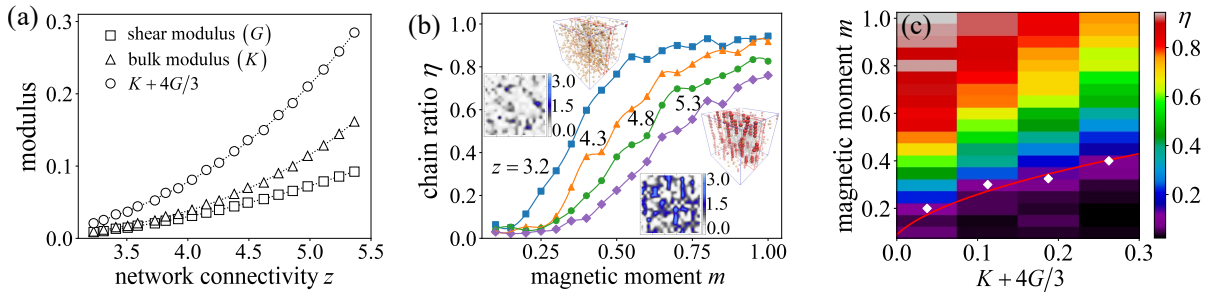


Figure 2: (a) Dependence of shear modulus  $G$  (squares), bulk modulus  $K$  (triangles) and  $K + 4G/3$  (circles) of the polymer gels on the network connectivity  $z$ . (b) Chain ratio as a function of the magnetic moments of the particles, in polymer networks with different connectivity. Insets denote the microscopic structures of the magnetic particles and the displacement field in the cross-sectional plane. (c) Chain ratio as a function of the magnetic moments and the network elasticity. Red line denote the physical conditions for the chain formation [Equation (5)], and the white diamonds correspond to simulation results of the critical chain ratio,  $\eta = 0.15$ .

network elasticity and the thermal fluctuations; this phenomenon resembles the clustering instability found in magnetic microswimmers, where the microswimmers can form clusters when magnetic dipole-dipole interactions dominate thermal fluctuations.<sup>51,52</sup> Due to the displacements of the magnetic particles in events of chain formations, the polymer network will be deformed with the local deformation field, as shown in the insets of Fig. 2(b). The chain ratio,  $\eta$ , defined as the ratio of the number of the magnetic particles forming the chains to the total number of the magnetic particles in the material, is introduced to characterize the amount of the micro-structures in the magnetic gel and also the relative strength of the magnetic dipole-dipole interactions over the network elasticity. We use the following criterion to identify if a particle belong to a chain: the distance to its nearest neighboring magnetic particle is less than  $2^{1/6}\sigma$ , and the angle between the direction of the magnetic moment and the position vector connected to its nearest neighboring particle is less than  $15^\circ$ . With the decrease in the network connectivity, i.e., the elastic moduli of the material, the chain ratio in magnetic gels of the particles with the same magnetic moments will increase.

By systematically changing the elastic moduli of the network and the magnetic moments of the particles, one can obtain the phase diagram showing the physical conditions for the

chain formation, as shown in Fig. 2(c). In simulations,  $\eta = 0.15$  is taken as the value of the chain ratio, for denoting the conditions of the chain formation, and one can observe from Fig. 2(c) that, for inclusions carrying large magnetic moments in soft polymer gels, they can easily form chain-like structures, coinciding with the theoretical conditions for the chain formation as derived in a previous work,<sup>24</sup>

$$\frac{\mu_0 n_0 m^2}{k_B T} > \frac{v_p}{k_B T} (K + 4G/3) + 1. \quad (5)$$

One can also check how the number density of magnetic particles in the prepared state,  $n_0$ , can influence the formation of the micro-structures in the gel. As shown in Fig. 3(a), the chain ratio is larger for systems characterized by a higher number density  $n_0$ , since the magnetic dipole-dipole interactions become stronger due to decreased distances between the magnetic particles. The physical conditions for the chain formation in the plane of  $(n_0, m)$  is provided in Fig. 3(b), which also agrees with our theoretical prediction.

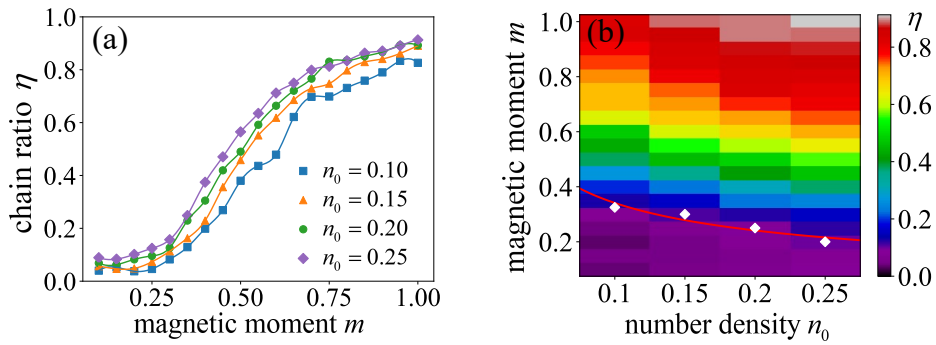


Figure 3: (a) Chain ratio  $\eta$  as a function of the magnetic moments  $m$  of the particles with different number density. (b) Dependence of the chain ratio on the magnetic moments and the number density of the magnetic particles. Red line denote the physical conditions for the chain formation [Equation (5)], and the white diamonds corresponds to simulation results of the critical chain ratio,  $\eta = 0.15$ .



## Macroscopic mechanical properties

The macroscopic mechanical properties of magnetic gels can become reinforced due to the formation of microscopic chains.<sup>4-7</sup> Here we investigate such effects by studying how magnetic gels consisting of particles carrying different magnetic moments can respond under shear deformations.

As shown in Fig. 4(a), the stress-strain relations of magnetic gels can change if the magnetic moments of the particles are different. The magnetic gels with chain formation exhibit obvious mechanical reinforcements (larger stresses compared with those without chain formation at same strains) and weak anisotropy, whose mechanical responses depend on the applied plane of the shear deformation. By defining the shear modulus of the material as  $G_{\alpha\beta} = \left. \frac{d\sigma_{\alpha\beta}}{d\varepsilon_{\alpha\beta}} \right|_{\varepsilon_{\alpha\beta}=0}$ , one can obtain the dependence of this modulus on the magnetic moments of the particles, as shown in Fig. 4(b). There is a weak effect of the anisotropy in the shear moduli appears at  $m_c \simeq 0.27$ , corresponding to the chain ratio as  $\eta = 0.15$  (same criterion as used for chain formation). Compared with the material containing inherent chains in its relaxed state (springs not deformed),<sup>32</sup> the anisotropy in the mechanical response here is weaker, since all the elastic springs are already distorted when the chains are formed in the current setup. More importantly, for  $m \leq m_c$ , the shear modulus remains almost unchanged by increasing the magnetic moments, but for  $m > m_c$ , the shear modulus increases quickly with the magnetic moments in an approximate form of

$$G_{\alpha\beta}(m) = G_{\alpha\beta,\infty} \frac{(m - m_c)^2}{a_m + (m - m_c)^2}, \quad (6)$$

where  $G_{\alpha\beta,\infty}$ ,  $a_m$  and  $m_c$  are fitting parameters for specific materials.<sup>6,32,53</sup>

By changing the network connectivity  $z$ , we can change the elasticity of the polymer gel in the prepared state, based on which one can compare the effects of magnetic interactions between the embedded particles and polymer elasticity in the mechanical properties of magnetic gels. As shown in Fig. 4(c), the contributions of magnetic interactions in the shear

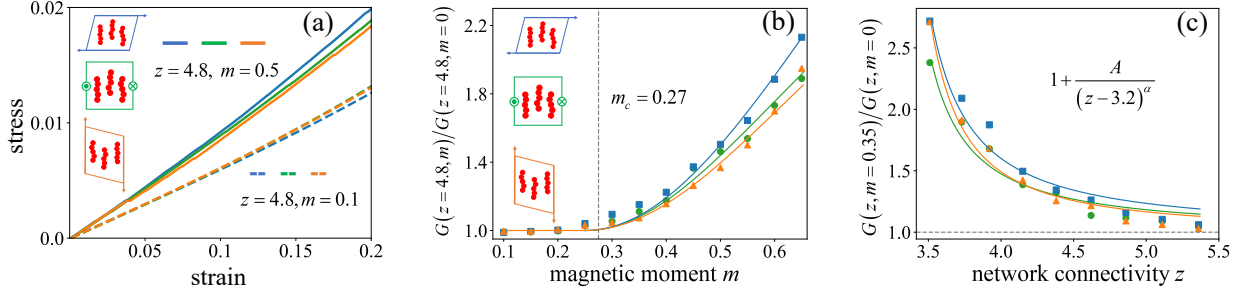


Figure 4: (a) Stress-strain relations of magnetic gels without (dash lines) and with (solid lines) chain formation, which undergoes the shear deformation in three orthogonal planes. (b) Dependence of the shear modulus  $G_{\alpha\beta}$  as a function of the magnetic moment of the particles, and lines fitted with Equation (6). (c) Comparison between the magnetic interactions and the polymer elasticity in terms of the shear modulus of the magnetic gels. Lines fitted with the function  $1 + A/(z - z_c)^\alpha$  with  $A$  and  $\alpha$  as fitting parameters.

modulus of magnetic gel where magnetic chains are formed, are significant for  $z \simeq z_c$ , which become less important by increasing the network connectivity due to the increased elasticity of the polymer network itself.

## Summary

We have studied the microscopic structure formation and the macroscopic mechanical responses of magnetic gels, by utilising the coarse-grained molecular dynamics simulations. By increasing the strength of the magnetic dipole-dipole interactions between the particles, the microscopic chain structures can form, which induces reinforced mechanical responses of the magnetic gels. This work can not only help to understand the connection between the microscopic structure and the macroscopic mechanical properties of the magnetic gels, but can also guide industrial fabrications of magnetic gels with desired mechanical responses and their controls by applying external magnetic fields for practical applications.

## Acknowledgments

F. M. acknowledges supports by National Natural Science Foundation of China (Grant No. 12275332, 12047503, and 12247130), Chinese Academy of Sciences, Max Planck Society (Max Planck Partner Group), Wenzhou Institute (Grant No. WIUCASQD2023009) and Beijing National Laboratory for Condensed Matter Physics (2023BNLCMPKF005). X. W. acknowledges supports from the China Postdoctoral Science Foundation (Grants No. 2023M743448) and the National Natural Science Foundation of China (Grants No. 12347170). P. T. acknowledges financial support from the European Research Council (Grant No. 811234) and from the Generalitat de Catalunya via the program “Icrea Academia”. The computations of this work were conducted on the HPC cluster of ITP-CAS.

## References

- (1) Brand, H.; Martinoty, P.; Pleiner, H. *Cross-Linked Liquid Crystalline Systems: From Rigid Polymer Networks to Elastomers*; 2011; pp 529–563.
- (2) Thévenot, J.; Oliveira, H.; Sandre, O.; Lecommandoux, S. Magnetic responsive polymer composite materials. *Chemical Society Reviews* **2013**, *42*, 7099.
- (3) Weeber, R.; Hermes, M.; Schmidt, A. M.; Holm, C. Polymer architecture of magnetic gels: a review. *Journal of Physics: Condensed Matter* **2018**, *30*, 063002.
- (4) Jolly, M. R.; Carlson, J. D.; Muñoz, B. C. A model of the behaviour of magnetorheological materials. *Smart Materials and Structures* **1996**, *5*, 607–614.
- (5) Collin, D.; Auernhammer, G. K.; Gavat, O.; Martinoty, P.; Brand, H. R. Frozen-In Magnetic Order in Uniaxial Magnetic Gels: Preparation and Physical Properties. *Macromolecular Rapid Communications* **2003**, *24*, 737–741.

- (6) Varga, Z.; Filipcsei, G.; Zrínyi, M. Smart composites with controlled anisotropy. *Polymer* **2005**, *46*, 7779–7787.
- (7) Varga, Z.; Filipcsei, G.; Zrínyi, M. Magnetic field sensitive functional elastomers with tuneable elastic modulus. *Polymer* **2006**, *47*, 227–233.
- (8) Raikher, Y. L.; Stolbov, O. Magnetodeformation effect in a ferroelastic material. *Technical Physics Letters* **2000**, *26*, 156–158.
- (9) Wang, Z.; Deng, B.; Yao, K. Physical model of plastic deformation on magnetization in ferromagnetic materials. *Journal of Applied Physics* **2011**, *109*.
- (10) Huang, S.; Pessot, G.; Cremer, P.; Weeber, R.; Holm, C.; Nowak, J.; Odenbach, S.; Menzel, A. M.; Auernhammer, G. K. Buckling of paramagnetic chains in soft gels. *Soft Matter* **2015**, *12*, 228–237.
- (11) Kim, Y.; Yuk, H.; Zhao, R.; Chester, S. A.; Zhao, X. Printing ferromagnetic domains for untethered fast-transforming soft materials. *Nature* **2018**, *558*, 274–279.
- (12) Alapan, Y.; Yasa, O.; Yigit, B.; Yasa, I. C.; Erkoc, P.; Sitti, M. Microrobotics and Microorganisms: Biohybrid Autonomous Cellular Robots. *Annual Review of Control, Robotics, and Autonomous Systems* **2019**, *2*, 205–230.
- (13) Kim, Y.; Zhao, X. Magnetic Soft Materials and Robots. *Chemical Reviews* **2022**, *122*, 5317–5364.
- (14) Gao, R.; Jiang, Y.; Zhao, Y. Magnetic field sensor based on anti-resonant reflecting guidance in the magnetic gel-coated hollow core fiber. *Optics letters* **2014**, *39*, 6293–6296.
- (15) Hankiewicz, J.; Celinski, Z.; Stupic, K.; Anderson, N.; Camley, R. Ferromagnetic particles as magnetic resonance imaging temperature sensors. *Nature communications* **2016**, *7*, 12415.

- (16) Gloag, L.; Mehdipour, M.; Chen, D.; Tilley, R. D.; Gooding, J. J. Advances in the application of magnetic nanoparticles for sensing. *Advanced Materials* **2019**, *31*, 1904385.
- (17) Shigetomi, S.; Takahashi, H.; Tsumori, F. Magnetic actuator using double network gel. *Journal of Photopolymer Science and Technology* **2020**, *33*, 193–197.
- (18) He, Y.; Tang, J.; Hu, Y.; Yang, S.; Xu, F.; Zrínyi, M.; Chen, Y. M. Magnetic hydrogel-based flexible actuators: A comprehensive review on design, properties, and applications. *Chemical Engineering Journal* **2023**, *462*, 142193.
- (19) Li, Y.; Huang, G.; Zhang, X.; Li, B.; Chen, Y.; Lu, T.; Lu, T. J.; Xu, F. Magnetic hydrogels and their potential biomedical applications. *Advanced Functional Materials* **2013**, *23*, 660–672.
- (20) Sung, B.; Kim, M.-H.; Abelmann, L. Magnetic microgels and nanogels: Physical mechanisms and biomedical applications. *Bioengineering & translational medicine* **2021**, *6*, e10190.
- (21) Veloso, S. R.; Andrade, R. G.; Castanheira, E. M. Review on the advancements of magnetic gels: towards multifunctional magnetic liposome-hydrogel composites for biomedical applications. *Advances in Colloid and Interface Science* **2021**, *288*, 102351.
- (22) Auernhammer, G. K.; Collin, D.; Martinoty, P. Viscoelasticity of suspensions of magnetic particles in a polymer: Effect of confinement and external field. *The Journal of Chemical Physics* **2006**, *124*, 204907.
- (23) Weeber, R.; Klinkigt, M.; Kantorovich, S.; Holm, C. Microstructure and magnetic properties of magnetic fluids consisting of shifted dipole particles under the influence of an external magnetic field. *The Journal of Chemical Physics* **2013**, *139*, 214901.
- (24) Junot, G.; Wei, X.; Ortín, J.; Golestanian, R.; Wang, Y.; Tierno, P.; Meng, F.

- Elastically-mediated collective organisation of magnetic microparticles. *Soft Matter* **2022**, *18*, 5171–5176.
- (25) Sunaryono; Taufiq, A.; Putra, E. G. R.; Okazawa, A.; Watanabe, I.; Kojima, N.; Rugmai, S.; Soontaranon, S.; Zainuri, M.; Triwikantoro; others Small-angle X-ray scattering study on PVA/Fe<sub>3</sub>O<sub>4</sub> magnetic hydrogels. *Nano* **2016**, *11*, 1650027.
- (26) Lawrence, M. B.; Abbas, S.; Aswal, V. Structure of polyvinyl alcohol-borax ferrogels: A small angle neutron scattering study. *Journal of Polymer Research* **2018**, *25*, 1–7.
- (27) Sorokina, O. N.; Kovarski, A. L.; Lagutina, M. A.; Dubrovskii, S. A.; Dzheparov, F. S. Magnetic nanoparticles aggregation in magnetic gel studied by electron magnetic resonance (EMR). *Applied Sciences* **2012**, *2*, 342–350.
- (28) Ramanujan, R.; Lao, L. The mechanical behavior of smart magnet–hydrogel composites. *Smart materials and structures* **2006**, *15*, 952.
- (29) Wu, J.; Gong, X.; Fan, Y.; Xia, H. Physically crosslinked poly (vinyl alcohol) hydrogels with magnetic field controlled modulus. *Soft Matter* **2011**, *7*, 6205–6212.
- (30) Ponton, A.; Bee, A.; Talbot, D.; Perzynski, R. Regeneration of thixotropic magnetic gels studied by mechanical spectroscopy: the effect of the pH. *Journal of Physics: Condensed Matter* **2005**, *17*, 821.
- (31) Zhang, G.; Zhang, Z.; Sun, M.; Yu, Y.; Wang, J.; Cai, S. The influence of the temperature on the dynamic behaviors of magnetorheological gel. *Advanced Engineering Materials* **2022**, *24*, 2101680.
- (32) Ivaneyko, D.; Toshchevikov, V.; Borin, D.; Saphiannikova, M.; Heinrich, G. Mechanical Properties of Magneto-Sensitive Elastomers in a Homogeneous Magnetic Field: Theory and Experiment. *Macromolecular Symposia* **2014**, *338*, 96–107.

- (33) Pessot, G.; Löwen, H.; Menzel, A. M. Dynamic elastic moduli in magnetic gels: Normal modes and linear response. *Journal of Chemical Physics* **2016**, *145*, 104904.
- (34) Jarkova, E.; Pleiner, H.; Müller, H. W.; Brand, H. R. Hydrodynamics of isotropic ferrogels. *Physical Review E - Statistical Physics, Plasmas, Fluids, and Related Interdisciplinary Topics* **2003**, *68*, 041706.
- (35) Romeis, D.; Toshchevikov, V.; Saphiannikova, M. Elongated micro-structures in magneto-sensitive elastomers: a dipolar mean field model. *Soft Matter* **2016**, *12*, 9364–9376.
- (36) Spieler, C.; Kästner, M.; Goldmann, J.; Brummund, J.; Ulbricht, V. XFEM modeling and homogenization of magnetoactive composites. *Acta Mechanica* **2013**, *224*, 2453–2469.
- (37) Wood, D. S.; Camp, P. J. Modeling the properties of ferrogels in uniform magnetic fields. *Physical Review E - Statistical, Nonlinear, and Soft Matter Physics* **2011**, *83*, 011402.
- (38) Cremer, P.; Heinen, M.; Menzel, A. M.; Löwen, H. A density functional approach to ferrogels. *Journal of Physics: Condensed Matter* **2017**, *29*, 275102.
- (39) Weeber, R.; Kantorovich, S.; Holm, C. Deformation mechanisms in 2D magnetic gels studied by computer simulations. *Soft Matter* **2012**, *8*, 9923–9932.
- (40) Pessot, G.; Weeber, R.; Holm, C.; Löwen, H.; Menzel, A. M. Towards a scale-bridging description of ferrogels and magnetic elastomers. *Journal of Physics: Condensed Matter* **2015**, *27*, 325105.
- (41) Weeber, R.; Kantorovich, S.; Holm, C. Ferrogels cross-linked by magnetic particles: Field-driven deformation and elasticity studied using computer simulations. *Journal of Chemical Physics* **2015**, *143*, 154901.

- (42) Shivers, J. L.; Feng, J.; Sharma, A.; MacKintosh, F. C. Normal stress anisotropy and marginal stability in athermal elastic networks. *Soft Matter* **2019**, *15*, 1666–1675.
- (43) Dagois-Bohy, S.; Tighe, B. P.; Simon, J.; Henkes, S.; Van Hecke, M. Soft-sphere packings at finite pressure but unstable to shear. *Physical review letters* **2012**, *109*, 095703.
- (44) Koeze, D.; Vågberg, D.; Tjoa, B.; Tighe, B. Mapping the jamming transition of bidisperse mixtures. *Europhysics Letters* **2016**, *113*, 54001.
- (45) Weeks, J. D.; Chandler, D.; Andersen, H. C. Role of Repulsive Forces in Determining the Equilibrium Structure of Simple Liquids. *The Journal of Chemical Physics* **1971**, *54*, 5237–5247.
- (46) Thompson, A. P.; Aktulga, H. M.; Berger, R.; Bolintineanu, D. S.; Brown, W. M.; Crozier, P. S.; in 't Veld, P. J.; Kohlmeyer, A.; Moore, S. G.; Nguyen, T. D.; Shan, R.; Stevens, M. J.; Tranchida, J.; Trott, C.; Plimpton, S. J. LAMMPS - a flexible simulation tool for particle-based materials modeling at the atomic, meso, and continuum scales. *Comp. Phys. Comm.* **2022**, *271*, 108171.
- (47) Grønbech-Jensen, N.; Farago, O. A simple and effective Verlet-type algorithm for simulating Langevin dynamics. *Molecular Physics* **2013**, *111*, 983–991.
- (48) Grønbech-Jensen, N. Complete set of stochastic Verlet-type thermostats for correct Langevin simulations. *Molecular Physics* **2020**, *118*, 8.
- (49) *See supplementary materials.*
- (50) Sharma, a.; Licup, a. J.; Jansen, K. a.; Rens, R.; Sheinman, M.; Koenderink, G. H.; MacKintosh, F. C. Strain-controlled criticality governs the nonlinear mechanics of fibre networks. *Nature Physics* **2016**, *12*, 584–587.
- (51) Meng, F.; Matsunaga, D.; Golestanian, R. Clustering of Magnetic Swimmers in a Poiseuille Flow. *Physical Review Letters* **2018**, *120*, 188101.



- (52) Meng, F.; Matsunaga, D.; Mahault, B.; Golestanian, R. Magnetic Microswimmers Exhibit Bose-Einstein-like Condensation. *Physical Review Letters* **2021**, *126*, 078001.
- (53) Varga, Z.; Filipcsei, G.; Zrínyi, M. Magnetic field sensitive functional elastomers with tuneable elastic modulus. *Polymer* **2006**, *47*, 227–233.